Electron. Mater. Lett., Vol. 9, No. 5 (2013), pp. 629-633
DOI: 10.1007/s13391-013-3002-9

Effect of Substitutional Doping on Temperature Dependent Electrical Parameters of Amorphous Se-Te Semiconductors

Neha Sharma,[1] Sunanda Sharda,[1] Dheeraj Sharma,[1] Vineet Sharma,[1] P.B. Barman,[1] S.C. Katyal,[2] Pankaj Sharma[1,*], and S. K. Hazra[1,*]

[1]Department of Physics and Materials Science, Jaypee University of Information Technology, Waknaghat, Solan, H.P.-173234, India
[2]Department of Physics and Materials Science, Jaypee Institute of Information Technology, Sec 128, Noida

(received date: 3 January 2013 / accepted date: 13 February 2013 / published date: 10 September 2013)

Steady state current-voltage characteristics of the amorphous $(Se_{80}Te_{20})_{98}Y_2$ (Y = Ag, Bi, Ge, Cd) semiconductors at different temperatures are reported. The measurements were performed using direct-current voltage bias to understand the basic conductivity mechanism and to evaluate the impact of each substituent on electrical response. The space charge limited conduction mechanism, and the density of states near Fermi level have been calculated. The difference in electrical response due to different substitutions in the glassy matrix is analyzed.

Keywords: amorphous materials, electrical properties, defects

1. INTRODUCTION

Chalcogenide glasses have emerged as prospective materials with their flexible synthesis approach for modern device applications.[1-5] These applications can be altered with impurities as per application requirement. Se based glasses have tremendous applications but problem lies in their thermal stability. Thermal stability can be improved by alloying Se with certain impurities e.g. Sb, Bi, Te etc.[6-8] But, still Binary chalcogenide glasses suffer from thermal stability, lower crystallization temperature and aging effects etc.[9-14] Properties of binary chalcogenide glasses have been improved by several researchers.[15-17] Current-voltage (*I-V*) characteristics for semiconductors (amorphous or crystalline) provide information regarding various junction properties *viz.* rectification ratio, diode quality factor, reverse saturation current, the series and the shunt resistance.[18] The electronic conductivities of chalcogenide glasses are governed by the nature of the chalcogen and for selenium the valence band bottom is formed by ion-pair states and the antibonding states represent the conduction band.[19] However, in a glass containing large amounts of Te, the band gap decreases (~1 eV), and the metallic character increases.[20,21] It has been reported that Se-Te alloys have more advantages than *a*-Se from the technological point of view due to their greater hardness, higher crystallization temperature, higher photo-sensitivity and smaller ageing effects.[22] Addition of Te brings about changes in Vander Waals bonds or interchain secondary bonds, because the Te atom is larger than the Se atom and has more electrons in its orbital. Therefore, one can argue that Te addition leads to increase in secondary bonding between chains. Te addition will also increase the valence alteration pair (VAP) type defects.[23]

I-V characteristics of amorphous semiconductors have been investigated by various researcher[24-26] and the conduction in amorphous semiconductors is mainly ascribed to the Space Charge Limited Conduction (SCLC) or Schottky emissions or Poole-Frenkel emissions. These semiconductors have intrinsic defects in the forbidden gap and the density of these defect states governs various physical properties. These defect states in material play an important role to determine device applications. Therefore, exact calculation of density of states is essential. These states can be calculated from the measurement of space charge limited current at high electric fields. In case of uniform traps, space charge limited conduction mechanism is used for the calculation of density of these states near the Fermi level.

Here, we report the electrical properties of amorphous Se-Te and their variation with different substituent (Ag, Bi, Ge, Cd). The current - voltage curves were analyzed to intrinsic resistivity, carrier concentration and to highlight a basic conduction mechanism in the material.

2. EXPERIMENTAL PROCEDURE

Glasses of $(Se_{80}Te_{20})_{98}Y_2$ (Y = Ag, Bi, Ge, Cd) compositions

*Corresponding author: pankaj.sharma@juit.ac.in
*Corresponding author: surajit.hazra@juit.ac.in
©KIM and Springer

have been synthesized using melt-quench technique. The detailed experimental procedure is given elsewhere.[20,21] X-ray diffraction technique is used to check the amorphous nature of samples. For electrical analysis (Keithley, model 6487) bulk samples were used in pellet (1 mm thickness, 10 mm diameter, load of ~10 ton) form. The pellets coated with silver paste were put on a specially designed sample holder, in which a vacuum of 10^{-3} mbar was maintained throughout the measurements. The experiments were performed at different ambient temperatures (35°C - 75°C) using a PID temperature controller. At least 10-minutes stabilization time was put into operation at each temperature before performing the *I-V* measurements.

3. RESULTS AND DISCUSSION

The application of sufficiently high electric fields to any material eventually results in deviations from linearity in the current-voltage (*I-V*) characteristics. Generally, two classes of explanations for such non-ohmic effects are accepted. Firstly, due to thermal effects, the electrons accelerated by the field always emit phonons in an attempt to return to equilibrium. Secondly, electronic effects introduce changes in response of the charge carriers to high applied fields. So, the electronic momentum is now altered due to the collision with generated phonons. Added to this, the high electric field strengthens the defect mobility and impurity scattering in these amorphous semiconductors. Therefore, the combined effect of temperature and high field is depicted as non-linearity in the *I-V* characteristics shown in Fig. 1. So, in the studied voltage range, current increases linearly for low voltage (0 - 20 V) and thereafter missed the linearity for all the studied samples. Probably the ohmic conduction mechanism is altered due to temperature and high bias voltages. Therefore, all subsequent analysis of grown samples was performed within 0 - 20 V range, which is

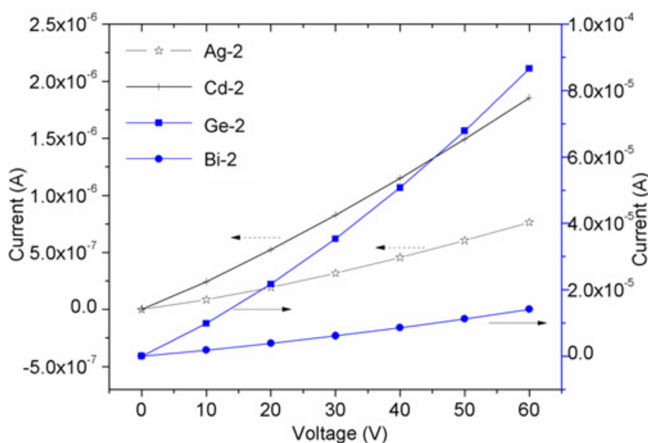

Fig. 1. Comparative *I-V* (0 - 60 volts) of amorphous $(Se_{80}Te_{20})_{98}Y_2$ (Y = Ag, Bi, Ge, Cd) semiconductors at room temperature.

normally the maximum range for all electrical applications. The maximum experimental temperature was restricted to 75°C, due to the stability consideration of amorphous phase. Basically, the stability is governed by the glass transition temperature. In our samples, this alarming temperature is 81°C maximum for Ge substitution.[27]

The excellent linearity in *I-V* characteristics, shown at all temperatures and for all samples (Fig. 2), clearly indicate the validity of Ohm's law. The d.c. resistance (R) is calculated from the slopes of *I-V* curves, and using the formulae ($R = \rho l/A$), the d.c. resisitivity (ρ), is calculated. Subsequent plot of ln(ρ) vs 1000/T is shown in Fig. 3(a). The plot of ln(ρ) vs. 1000/T clearly indicates the semiconducting nature of the samples. The resistivity is decreasing with increase in temperature for all samples. The slope of the linear variation in resistivity plot is used to calculate activation energy. The activation energy (E_a) corresponding to charge transfer and the intrinsic resistivity ρ_0 are calculated from

$$\rho = \rho_0 e^{E_a/2kT}. \tag{1}$$

The charge carrier concentration for investigated samples are calculated using the relation:[28]

$$n_\sigma = 2\left(\frac{2\pi m k_B T}{h^2}\right)^{3/2} \exp\left(-\frac{E_a}{2k_B T}\right). \tag{2}$$

Figure 3(b) clearly points that with increasing temperature, the charge carrier concentration increases. Charge carrier concentration is found to be maximum for Ag substitution and varies as $(n_\sigma)_{Ag} > (n_\sigma)_{Bi} > (n_\sigma)_{Ge} > (n_\sigma)_{Cd}$. This variation can be explained on the basis of decrease in activation energy (Fig. 3(c)). A decrease in activation energy also accounts for an increase in the localized states and further increasing localized states will lead to a decrease in optical band gap. The optical band gap results support our present research.[29]

For a uniform distribution of localized states having density g, current I, at voltage V, the conduction mechanism could be understood by using space charge limited conduction (SCLC).[30]

$$I = 2eA\mu n_o (V/d)\exp(SV) \tag{3}$$

where e electronic charge, A area of cross section, μ permeability, n_o density of free charge carriers, d electrode spacing, and S is given by:

$$S = \frac{2\varepsilon_r \varepsilon_o}{egkTd^2} \tag{4}$$

where ε_r is the static dielectric constant. The values of ε_r are $(Se_{80}Te_{20})_{100-x}Ag_2 = 10.64$, $(Se_{80}Te_{20})_{100-x}Bi_2 = 9.847$, $(Se_{80}Te_{20})_{100-x}Cd_2 = 6.76$, $(Se_{80}Te_{20})_{100-x}Ge_2 = 10.517$;[29] ε_o is permittivity of free space, k is Boltzmann constant. The

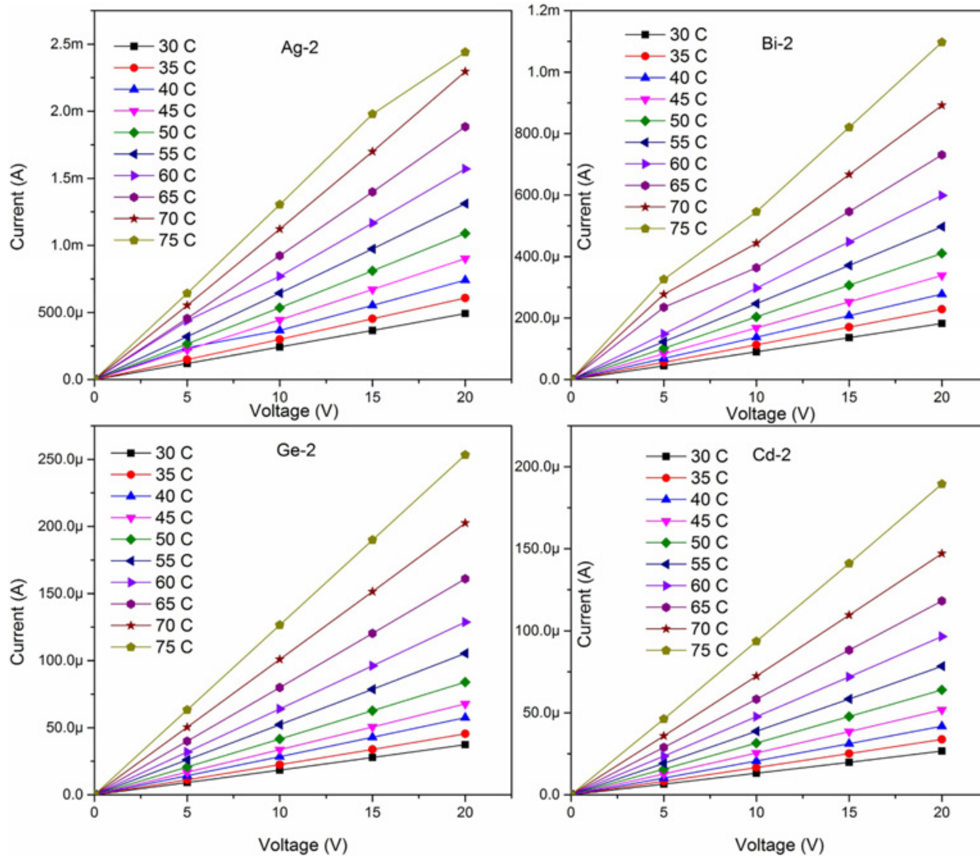

Fig. 2. Comparative *I-V* of the linear zone (0 - 20 volts) for amorphous $(Se_{80}Te_{20})_{98}Y_2$ (Y = Ag, Bi, Ge, Cd) semiconductors at different temperatures.

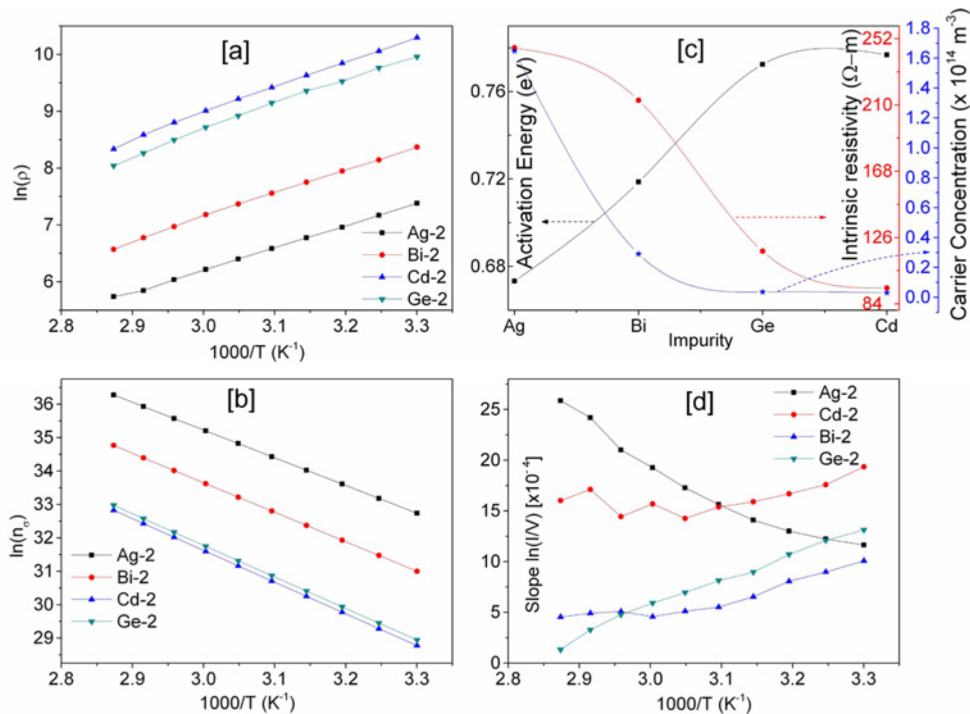

Fig. 3. For amorphous $(Se_{80}Te_{20})_{98}Y_2$ (Y = Ag, Bi, Ge, Cd) semiconductors at different temperatures; (a) Resistivity variation, (b) Charge carrier concentration variation, (c) Comparative plot of semiconducting parameters, (d) Slope of (ln(*I/V*) vs. V) vs. (1000/*T*).

value of S is obtained from the slope of ln(I/V) vs. V plot (Fig. 4). The obtained slopes are plotted vs. (1000/T) in Fig. 3(d).

From Fig. 3(d), it is clear that for $(Se_{80}Te_{20})_{100-x}Ag_2$ sample, slope is negative and increases with an increase in temperature. However, for other three samples, slope is decreasing with increase in temperature; this implies that SCLC mechanism is not applicable for $(Se_{80}Te_{20})_{100-x}Ag_2$. The SCLC mechanism is a bulk and thin film phenomenon. However, it is more prominent in thin films. Kumar *et al.*[31] reported the observation of SCLC mechanism for minimum silver substitution (with $Se_{92}Te_4Ag_4$ films). In our studies with bulk samples, the silver concentration is much lower (2 at. %) than that reported by Kumar *et al.*[31] So, it is obvious that such low concentration of silver in bulk samples will not favor SCLC mechanism. Comparing the electronegativity values of Se (2.55), Te (2.1), Bi (2.02), Ge (2.01), Cd (1.69), one can expect that when dopants like Bi, Ge, and Cd are introduced in Se-Te matrix, positively charged defects will be created.[30] The addition of electropositive elements to Se-Te alloy (having higher electronegativity) creates defect states within the forbidden gap. This can also be correlated with the activation energy values. Compositions with higher defect states will have lower activation energy. Therefore it is evident from the Fig. 3(c) that Bismuth addition will have higher defect states compared to Germanium and Cadmium. Further, the calculated electronegativity values (Table 1) also shows a decreasing order.[32]

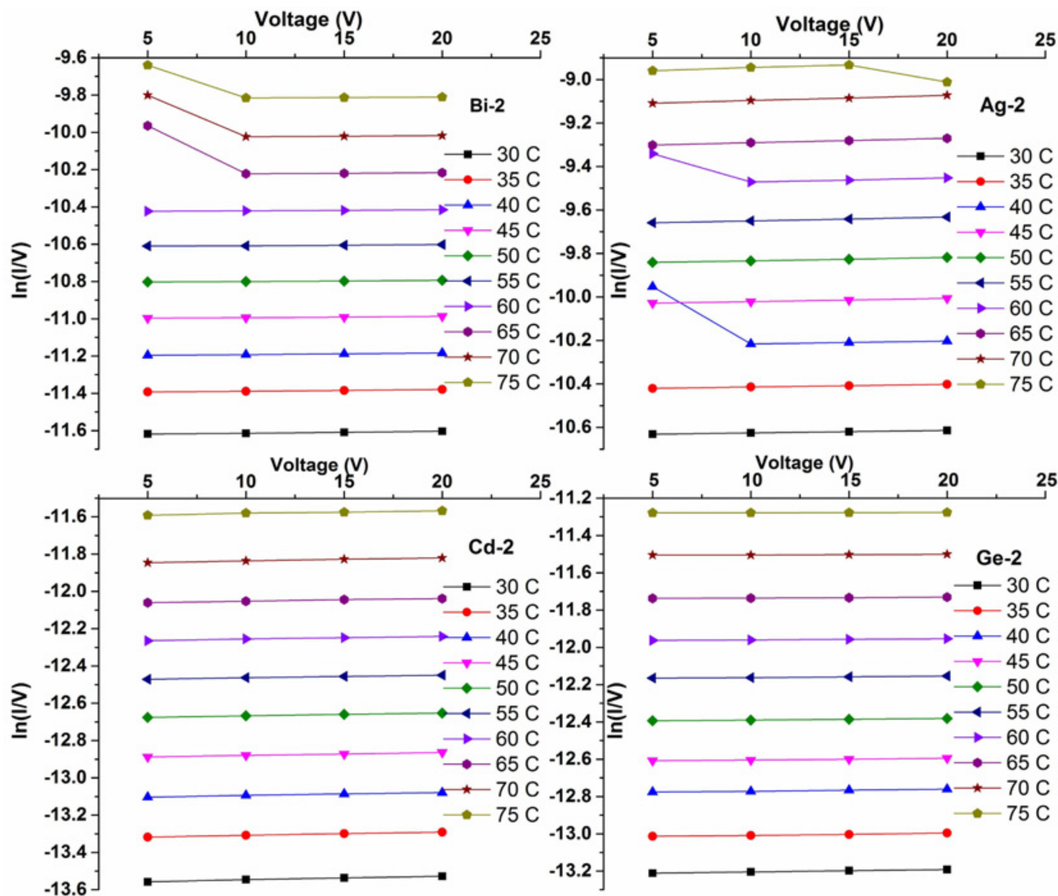

Fig. 4. ln(I/V) vs. V plot for $(Se_{80}Te_{20})_{98}Y_2$ (Y = Ag, Bi, Ge, Cd) semiconductors at different temperatures.

Table 1. Values of charge carrier concentration at 30°C and density of states (g).

Alloy	Concentration of charge carriers at 30°C (m^{-3})	Slope (from Fig. 3(d))	g ($eV^{-1}m^{-3}$)	Electronegativity
$(Se_{80}Te_{20})_{98}Ag_2$	1.648×10^{14}	-	-	-
$(Se_{80}Te_{20})_{98}Bi_2$	2.905×10^{13}	1.9334×10^{-3}	1.63×10^{18}	2.4434
$(Se_{80}Te_{20})_{98}Ge_2$	3.704×10^{12}	2.6563×10^{-3}	1.27×10^{18}	2.4431
$(Se_{80}Te_{20})_{98}Cd_2$	3.141×10^{12}	1.8647×10^{-3}	1.16×10^{18}	2.4346

The slope of the linear zone (3.03 - 3.3 K^{-1}) of Fig. 3(d) is used to calculate the values of g using Eq. (4) (Table 1). The samples following SCLC probably have large number of localized defect states and these states act as trapping centers for the charge carriers. As a matter of fact, charge accumulation occurs between the electrodes after the field is applied. This charge build up is responsible for SCLC mechanism in these samples. Comparing the values of g for the studied samples, it is obvious, that Bismuth substitution is providing maximum number of defect states between the valence and conduction band. This implies that the electronic transition is now limited to small energy barriers. So, the activation energy for Bi substituted sample must be lowest (Fig. 3(c)). Similar studies were reported by Sharma *et al.*, $(Se_{0.75}Te_{0.15}Sn_{0.10})$[25] and Khan *et al.* $(Se_{80}Te_{18}Pb_2)$[24] with g values 2.34×10^{14} and 2.13×10^{13} $eV^{-1}cm^{-3}$ respectively.

4. CONCLUSIONS

Current-Voltage characteristics for amorphous $(Se_{80}Te_{20})_{98}Y_2$ (Y = Ag, Bi, Cd Ge) semiconductors reveal linearity upto 20 V. In linear region, we have calculated the intrinsic resistivity, activation energy, and carrier concentration. The activation energy (E_a) follows the inequality: $(E_a)_{Ag} < (E_a)_{Bi} < (E_a)_{Ge} < (E_a)_{Cd}$. The intrinsic resistivity and the carrier concentration have opposite trend: $(n_\sigma)_{Ag} > (n_\sigma)_{Bi} > (n_\sigma)_{Ge} > (n_\sigma)_{Cd}$; $(\rho_o)_{Ag} > (\rho_o)_{Bi} > (\rho_o)_{Ge} > (\rho_o)_{Cd}$. Further, the space charge limited conduction (SCLC) mechanism is evident in Bi, Ge, Cd substitutions; however, silver substitution does not show SCLC. The calculated density of states is highest for bismuth substitution; this implies large number of defect states in the forbidden gap which lowers its energy gap.

REFERENCES

1. K. Nakayama, T. Sato, P. Richard, T. Kawahara, Y. Sekiba, T. Qian, G. F. Chen, J. L. Luo, N. L. Wang, H. Ding, and T. Takahashi, *Phys. Rev. Lett.* **105**, 197001-4 (2010).
2. D. S. Jeong, R. Thomas, R. S. Katiyar, J. F. Scott, H. Kohlstedt, A. Petraru, and C. S. Hwang, *Rep. Prog. Phys.* **75**, 076502 (2012).
3. K.-B. Song, S.-S. Lee, K.-A. Kim, J.-D. Suh, J.-H. Kim, T.-S. Lee, B.-K. Cheong, and W.-M. Kim, *Appl. Phys. Lett.* **90**, 263510 (2007).
4. E. Güneri and A. Kariper, *Electron. Mater. Lett.* **9**, 13 (2013).
5. S. J. Park, S.-J. Park, D. B. Park, M. An, M.-H. Cho, J. G. Kim, H. D. Na, S. H. Park, and H. C. Sohn, *Electron. Mater. Lett.* **8**, 175 (2012)
6. D. Tonchev and S. O. Kasap, *J. Non-Cryst. Solids* **248**, 28 (1999).
7. S. Srivastava, M. Zulfequar, and A. Kumar, *Chalcogenide Lett.* **6**, 403 (2009).
8. N. Mehta, D. Kumar, and A. Kumar, *Phys. Status Solidi A* **204**, 3108 (2007).
9. S. Gu, Z. Ma, H. Tao, C. Lin, H. Hu, X. Zhaoa, and Y. Gong, *J. Phys. Chem. Solids* **69**, 97 (2008).
10. S. Srivastava, N. Mehta, C. P. Singh, R. K. Sukla, and A. Kumar, *Physica B* **403**, 2910 (2008).
11. A. K. Varshneya and D. J. Mauro, *J. Non-Cryst. Solids* **353**, 1291 (2007).
12. S. M. El-Sayed, *Appl. Surface Science* **253**, 7089 (2007).
13. M .N. Kozicki and M. Mitkova, *J. Non-Cryst. Solids* **352**, 567 (2006).
14. E. R. Shaaban, *Physica B* **373**, 211 (2006).
15. V. Vassilev, S. Parvanov, T. Hristova-Vasileva, V. Parvanova, and D. Ranova, *Mater. Chem. Phys.* **105**, 53 (2007).
16. A. Ahamd, S. A. Khan, Z. H. Khan, M. Zulfequar, K. Singha, and M. Husain, *Physica B* **382**, 92 (2006).
17. M. M. Imran, D. Bhandari, and N. S. Saxena, *Mater. Sci. Eng. A* **292**, 56 (2000).
18. M. M. El-Nahass, H. E. A. El-Sayed, and A. M. A. El-Barry, *Solid-State Electronics* **50**, 355 (2006).
19. N. Mehta, A. Dwivedi, R. Arora, S. Kumar, and A. Kumar, *Bull. Mater. Sci.* **28**, 579 (2005).
20. P. Sharma and S. C. Katyal, *Thin Solid Films* **517**, 3813 (2009).
21. P. Sharma and S. C. Katyal, *Thin Solid Films* **515**, 7966 (2007).
22. B. E. Springett, *Phosphorus Sulfur and the Related Elements* **38**, 341 (1988).
23. C. A. Angell, *Chem. Rev.* **90**, 523 (1990).
24. M. A. Majeed Khan, M. Zulfequar, and M. Husain, *Mater. Lett.* **57**, 2894 (2003).
25. N. Sharma and S. Kumar, *Turk. J. Phys*, **31**, 161 (2007).
26. M. Nardone, M. Simon, I. V. Karpov, and V. G. Karpov, *J. Appl. Phys.* **112**, 071101 (2012).
27. M. Kapoor and N. Thakur, *Integrated Ferroelectrics: An International Journal* **118**, 53 (2010).
28. V. Sharma, A. Thakur, N. Goyal, G. S. S. Saini, and S. K. Tripathi, *Semicond. Sci. Technol.* **20**, 103 (2005).
29. Mainika, P. Sharma, S. C. Katyal, and N. Thakur, *J. Non-Oxide Glasses* **1**, 90 (2009).
30. M. A. M. Khan, M. Zulfequar, and M. Husain, *J. Mater. Sci. Lett.* **22**, 61 (2003).
31. S. Kumar, M. Husain, and M. Zulfequar, *J. Optoelectron. Biomedical Mater.* **1**, 147 (2009).
32. R. T. Sanderson, *Inorganic Chemistry,* p. 194, Affiliated East West Press PUT, New Delhi (1971).